

Interpretation of VLBI Results in Geodesy,
Astrometry and Geophysics

Extending the ICRF above S/X-band: X/Ka-band Global Astrometric Results

Christopher Jacobs¹, Ojars Sovers²

¹⁾ *Jet Propulsion Laboratory, California Institute of Technology, USA*

²⁾ *Remote Sensing Analysis Systems Inc., USA*

Abstract. In order to extend the International Celestial Reference Frame from its S/X-band (2.3/8.4 GHz) basis to a complementary frame at X/Ka-band (8.4/32 GHz), we began an ongoing series of X/Ka observations starting in mid-2005 using NASA's Deep Space Network (DSN) radio telescopes. This paper will report global astrometric results from the first 33 sessions. These sessions covered the full 24 hours of right ascension and declination down to -45 degrees. Our analysis produced a radio frame of 318 sources with median formal position uncertainties of ≈ 0.25 mas. A comparison of our X/Ka-band frame against S/X-band shows WRMS differences of ≈ 0.25 mas. These differences include zonal errors the largest of which is a trend vs. declination. We will discuss our error budget including systematic errors from limited sensitivity, mis-modelling of the troposphere, and uncalibrated instrumental effects. We will discuss our plan for addressing the current limiting errors and the resulting prospects for improved accuracy over the next few years.

1. Introduction

For almost three decades now, radio frequency work in global astrometry, geodesy, and deep space navigation has been done at S/X-band (2.3/8.4 GHz). While this work has been tremendously successful in producing 100 μ as level global astrometry [3] and sub-cm geodesy, developments made over the last decade have made it possible to consider the merits of moving to a new set of dual-band frequencies. In this paper we present global astrometric results from X/Ka-band (8.4/32 GHz) observations. Complementary single-band results at 24 and 43 GHz are presented by Lanyi (this volume).

Moving the observing frequencies up by approximately a factor of four has several advantages. For our work in the Deep Space Network, the driver is the potential for higher telemetry data rates to and from probes in deep space. Other advantages include: 1) the spatial distribution of flux becomes significantly more compact lending hope that the positions will be more stable

over time, 2) Radio Frequency Interference (RFI) at S-band would be avoided, 3) ionosphere and solar plasma effects on group delay and signal coherence are reduced by a factor of 15!

While these are very significant advantages, there are also disadvantages. The change from 2.3/8.4 GHz to 8.4/32 GHz moves one closer to the water vapor line at 22 GHz and thus increases the system temperature from a few Kelvins per atmospheric thickness up to 10-15 Kelvins per atmosphere or more. Thus one becomes much more sensitive to weather. Furthermore, the sources themselves are in general weaker and many sources are resolved. Also, with the observing wavelengths shortened by a factor of 4, the coherence times are shortened so that practical integration times are a few minutes or less-even in relatively dry climates. The shorter wavelengths also imply that the antenna pointing accuracy requirements must be tightened by the same factor of 4. The combined effect of these disadvantages is to lower the system sensitivity. Fortunately, recent advances in recording technology (cf. Whitney, this volume) make it feasible and affordable to offset these losses in sensitivity by recording more bits. Thus while the X/Ka results presented in this paper used the same overall bit rate as previous S/X work, efforts are now underway to increase our bit rate by a factor of 4 to 8 within the next few years.

This paper is organized as follows: We will describe the observations, modelling, and present the results. Next, we will estimate the accuracy by comparing to a recent S/X celestial reference frame. This will be complemented by a discussion of the error budget. Finally, we will provide conclusions and anticipated directions for further research.

2. Observations and Modelling

The results presented here are from 33 VLBI observing sessions of 24 hour duration done from July 2005 until Jan. 2008 using NASA's Deep Space Stations (DSS) 25 or 26 in Goldstone, California to either DSS 34 in Tidbinbilla, Australia or DSS 55 outside Madrid, Spain to form interferometric baselines of 10,500 and 8,400 km length, respectively.

We recorded VLBI data simultaneously at X (8.4 GHz) and Ka-band (32 GHz) sampling each band at a rate of 56 Mbps. Each band's 7 channels (each ± 2 MHz) spanned a bandwidth of ≈ 360 MHz. The data were filtered, sampled, and recorded to tape using the MKIV VLBI system. The data were then correlated with the JPL BlockII correlator [5]. Fringe fitting was done with the FIT fringe fitting software [2]. This procedure resulted in 6363 pairs of group delay and phase rate measurements covering the full 24 hours of right ascension and declinations down to -45 deg. Each observation was approximately 2 minutes in duration.

The above described set of observations were then modelled using the MODEST software [6]. A priori Earth orientation was fixed to the MHB nutation model [4] and empirically determined UT1-UTC and Polar Motion from the Space 2006 series [1]. The celestial frame was aligned to the ICRF [3] by fixing

the RA and Dec of OJ 287 and the declination of CTD 20. Station locations were estimated, but velocities were fixed to a decades-long S/X-band VLBI estimates.

3. Results

In all, we detected 318 extragalactic radio sources which covered the full 24 hours of RA and declinations down to -45° . In Fig. 1 below, these sources are plotted using an Aitoff projection to show their locations on the sky. RA=0 is at the center. The ecliptic plane is shown by a dashed line and the Galactic plane is indicated as a black line shaped approximately like an Ω . The sources are coded according to their $1\text{-}\sigma$ formal declination uncertainties with the value ranges indicated in the figure's legend. Note that the declination precision decreases as one moves toward the south. This is a result of having significantly less data on the California to Australia baseline combined with the need to observe sources closer to the horizon as declination moves south thus incurring greater error from higher system temperatures and tropospheric mismodelling.

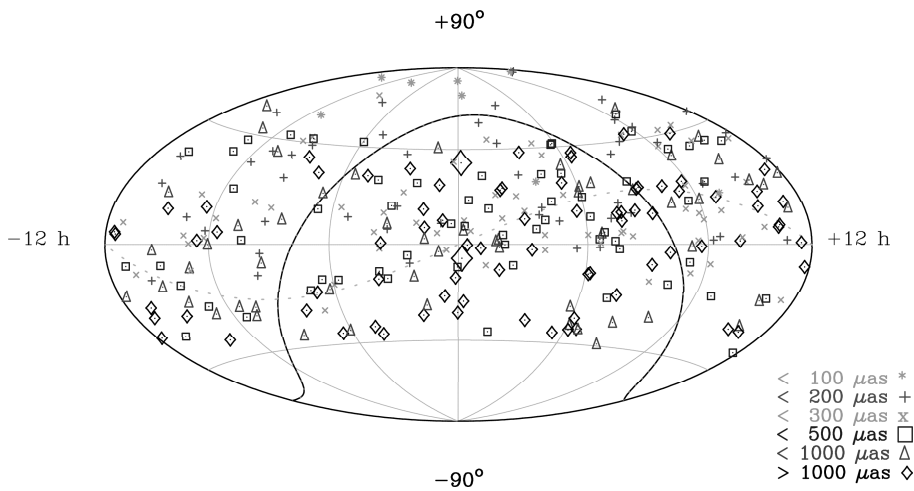


Figure 1. Distribution of 318 X/Ka-band sources detected to date. Symbols indicate $1\text{-}\sigma$ formal declination uncertainties with size bins defined in the legend at lower right. $(\alpha, \delta) = (0, 0)$ is at the center.

4. Accuracy and Zonal Errors

Experience shows that formal uncertainties tend to underestimate true errors. External estimates of errors were obtained by comparing our X/Ka-band RA and declinations to estimates from our analysis of S/X data covering the

period 1978–2007. For 255 common sources, the weighted RMS (WRMS) differences are $241 \mu\text{as}$ in RA $\cos(\text{dec})$ and $290 \mu\text{as}$ in declination. These differences reveal decreasing accuracy RA and declination as one moves south.

In astrometry, it is usually much easier to measure the relative positions of nearby sources than to accurately measure sources that are separated by long arcs. In order to investigate this tendency, we calculated for both X/Ka and S/X the arclengths between all pairs of sources, binned them in 5 deg bins and then differenced the arcs. We then took the mean arclength difference for each bin. As expected, arclengths agree better for short arcs and gradually worsen as arcs grow longer out to a mean difference of $70 \mu\text{as}$ at arcs of 90 deg. This is one measure of the level of zonal errors in our comparison.

5. Error Budget and Conclusions

Having assessed the size of errors in our positions using the much larger S/X data set as a standard of accuracy, we now discuss the major contributions to the errors of the X/Ka measurements: SNR, instrumentation, and troposphere. Fig. 2 shows the weighted RMS group delay vs. \log_{10} of the Ka-band SNR. We conclude that for $\text{SNR} < 30$, the thermal error dominates the error budget. For higher SNRs, troposphere and instrumentation errors become important. Binning of WRMS delay vs. airmass thickness shows that troposphere is not the dominant error due to the generally low SNRs just mentioned. However, the phase rates (which carry much less weight in the fit) are dominated by errors from tropospheric mismodelling, thus hinting that troposphere will become more important as our SNR improves. The last major category of errors comes from un-calibrated instrumentation. A proto-type phase calibrator has been developed for calibrating from the feed to the digitizer. Test data indicate an approximately diurnal instrumental effect with $\approx 180 \text{ ps}$ RMS. Although the data themselves can be used to partially parametrize this effect, we believe that phase calibrators will be needed in order to achieve accuracy of better than $200 \mu\text{as}$ in a timely manner.

Conclusions: The S/X-band ICRF has now been extended to the four times higher frequency of X/Ka-band (8.4/32 GHz). A total of 318 sources have been successfully detected. For the 255 sources with sufficient overlap to warrant comparison to S/X results, we find positional agreement of $241 \mu\text{as}$ in RA $\cos(\text{declination})$ and $290 \mu\text{as}$ in declination with zonal errors of $70 \mu\text{as}$.

As positive as these results are, we note that our X/Ka work still relies on ongoing S/X work for various geophysical models (nutations, precession, UT1–UTC). Thus it will be premature to speak of ending S/X observations for many years to come. Our current limiting errors are SNR and lack of instrumental phase calibration. We plan to address the SNR issue by increasing the recorded bit rate by a factor of 4–8. A proto-type phase calibrator has been built and we are seeking funding for operational units. If these goals are achieved, we believe that we can achieve $200 \mu\text{as}$ or better by 2010.

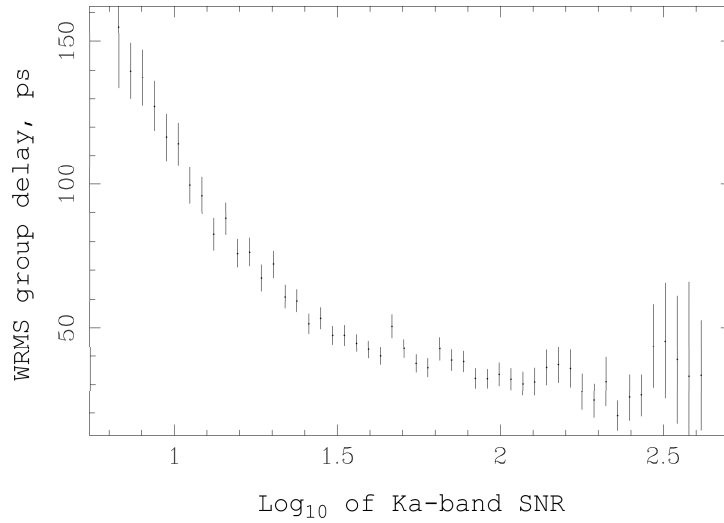


Figure 2. The WRMS residual group delay vs. the log₁₀ of the Ka-band SNR. Note the noise floor of ≈ 30 ps as other error sources such as troposphere and instrumentation begin to dominate once the SNR becomes > 30

Acknowledgements

The research described in this paper was performed at the Jet Propulsion Laboratory of the California Institute of Technology, under a contract with the National Aeronautics and Space Administration.

References

- [1] Gross, R.S. SPACE2006, JPL Publ., 07-5, Pasadena CA, 2007.
- [2] Lowe, S.T. JPL Publ., 92-7, Pasadena, CA, 1992.
- [3] Ma, et al. The ICRF as Realized by VLBI. A.J., 116, 516, 1998.
- [4] Mathews, Herring, Buffet. JGR, 107, B4, 2002.
- [5] O'Connor, T. BlockII Correlator. JPL internal publication. Pasadena CA, 1987.
- [6] Sovers, Fanelow, Jacobs. Rev. Mod. Phys., 70, 4, 1998.